Annals of Botany **114**: 1497–1505, 2014
doi:10.1093/aob/mcu185, available online at www.aob.oxfordjournals.org

ANNALS OF BOTANY
Founded 1887

PART OF A SPECIAL ISSUE ON FLOWER DEVELOPMENT

ULTRAPETALA1 and LEAFY pathways function independently in specifying identity and determinacy at the Arabidopsis floral meristem

Julia Engelhorn[1,2,3,4], Fanny Moreau[1,2,3,4], Jennifer C. Fletcher[5] and Cristel C. Carles[1,2,3,4,*]

[1]*Université Grenoble Alpes, UMR5168, F-38041 Grenoble, France,* [2]*CNRS, UMR5168, F-38054 Grenoble, France,* [3]*CEA, iRTSV, Laboratoire Physiologie Cellulaire et Végétale, F-38054 Grenoble, France,* [4]*INRA, F-38054 Grenoble, France and* [5]*Plant Gene Expression Center, USDA–ARS/University of California, Berkeley, 800 Buchanan Street, Albany, CA 94710, USA*
**For correspondence. E-mail Cristel.carles@ujf-grenoble.fr*

Received: 7 May 2014 Returned for revision: 13 June 2014 Accepted: 14 July 2014 Published electronically: 6 October 2014

• **Background and Aims** The morphological variability of the flower in angiosperms, combined with its relatively simple structure, makes it an excellent model to study cell specification and the establishment of morphogenetic patterns. Flowers are the products of floral meristems, which are determinate structures that generate four different types of floral organs before terminating. The precise organization of the flower in whorls, each defined by the identity and number of organs it contains, is controlled by a multi-layered network involving numerous transcriptional regulators. In particular, the AGAMOUS (AG) MADS domain-containing transcription factor plays a major role in controlling floral determinacy in *Arabidopsis thaliana* in addition to specifying reproductive organ identity. This study aims to characterize the genetic interactions between the ULTRAPETALA1 (ULT1) and LEAFY (LFY) transcriptional regulators during flower morphogenesis, with a focus on *AG* regulation.
• **Methods** Genetic and molecular approaches were used to address the question of redundancy and reciprocal interdependency for the establishment of flower meristem initiation, identity and termination. In particular, the effects of loss of both ULT1 and LFY function were determined by analysing flower developmental phenotypes of double-mutant plants. The dependency of each factor on the other for activating developmental genes was also investigated in gain-of-function experiments.
• **Key Results** The ULT1 and LFY pathways, while both activating *AG* expression in the centre of the flower meristem, functioned independently in floral meristem determinacy. Ectopic transcriptional activation by ULT1 of *AG* and *AP3*, another gene encoding a MADS domain-containing flower architect, did not depend on LFY function. Similarly, LFY did not require ULT1 function to ectopically determine floral fate.
• **Conclusions** The results indicate that the ULT1 and LFY pathways act separately in regulating identity and determinacy at the floral meristem. In particular, they independently induce *AG* expression in the centre of the flower to terminate meristem activity. A model is proposed whereby these independent contributions bring about a switch at the *AG* locus from an inactive to an active transcriptional state at the correct time and place during flower development.

Key words: Organogenesis, flower meristem identity, flower morphogenesis, flower determinacy, flower development, *Arabidopsis thaliana*, activation of transcription, ULTRAPETALA1, ULT1, LEAFY, LFY, MADS domain-containing proteins, AGAMOUS, trithorax group, trxG, chromatin.

INTRODUCTION

The appearance of the flower structure during plant evolution represents a success that places angiosperms among the most diverse groups on the planet, representing over 90 % of plant species (~300 000 existent angiosperm species). The success of the flower is inseparable from its function in the transmission of gametes. Thanks to the plasticity of development, the consolidation of specialized reproductive organs inside a single structure – the angiosperm flower – has led to the conquest of different ecological niches on land (Krizek and Fletcher, 2005). Although some taxa, such as orchids and the passion flower, have specific floral organ types, flower structure is extremely uniform within angiosperms, with its arrangement in concentric whorls composed of four types of organs: sepals, petals, stamens and carpels. This uniformity of flower patterning is also found at the molecular regulatory level.

The current model explains how the combination of A, B, C and E activities, provided predominantly by MADS domain-containing transcription factors, establishes the identity of the four floral organ types (O'Maoiléidigh *et al.*, 2013). In *Arabidopsis thaliana*, A function in whorls 1 and 2 is conferred by the *APETALA1* (*AP1*) and *AP2* genes, B function in whorls 2 and 3 is conferred by the *AP3* and *PISTILLATA* (*PI*) genes, and C function in whorls 3 and 4 is conferred by the sole *AGAMOUS* (*AG*) gene. Reverse genetics studies (Pelaz *et al.*, 2000; Ditta *et al.*, 2004) revealed that E function is conferred by the MADS domain-containing proteins SEPALLATA1 (SEP1) to SEP4, which operate redundantly as cofactors for the ABC proteins (Irish, 2010). Since then, the organization of

MADS domain-containing proteins in complexes has been studied extensively (Smaczniak *et al.*, 2012*a*, *b*).

The Arabidopsis LEAFY (LFY) transcription factor (TF) was identified as a master regulator for the ABCE functions and is indispensable for flower development. In *lfy* loss-of-function mutants, the flowers are replaced by cauline leaves, with shoots or shoot/flower intermediates developing at their axils (Weigel *et al.*, 1992). LFY gain-of-function phenotypes revealed a function in flower meristem initiation, as plants carrying a *CaMV35S::LFY* construct produce ectopic flowers in the axils of rosette and cauline leaves (Weigel and Nilsson, 1995). Moreover, in these plants the main shoot terminates in a solitary flower, indicating a function in stem cell termination in reproductive meristems.

In Arabidopsis, termination of stem cell activity in flower buds relies on a temporal negative feedback loop (Lenhard *et al.*, 2001; Lohmann *et al.*, 2001) involving the stem cell maintenance factor WUSCHEL (WUS) (Laux *et al.*, 1996; Mayer *et al.*, 1998) and the floral MADS domain-containing protein AG. Over a decade ago, studies showed that AG terminates floral stem cell maintenance by repressing *WUS* expression (Lenhard *et al.*, 2001; Lohmann *et al.*, 2001). More recently, the molecular mechanism for this regulation was resolved, in which AG represses *WUS* expression by two distinct mechanisms. Early in floral development AG directly represses *WUS* expression by recruiting Polycomb group (PcG) complexes for chromatin silencing at the locus (Liu *et al.*, 2011). Subsequently, AG activates the C2H2 zinc-finger-encoding *KNUCKLES* (*KNU*) gene, which in turn directly or indirectly represses *WUS* expression (Sun *et al.*, 2009). Genetic studies are consistent with KNU and PcG acting downstream of AG and in parallel to each other in terminating floral stem cell maintenance. Interestingly, AG can also function antagonistically to the PcG complex in regulating *KNU*, causing its eviction from the locus for transcriptional activation (Sun *et al.*, 2014).

Activation of floral organ identity genes in the different areas of the floral bud is regulated by the coordinated activities of *LFY*, which is expressed throughout the floral meristem, and co-regulators with more specific expression patterns (Parcy *et al.*, 1998). In the case of C function, the *AG* gene is activated by the synergistic actions of LFY and the WUS homeodomain transcription factor, the DNA binding motifs of which are juxtaposed in the *AG* regulatory sequences (Lenhard *et al.*, 2001; Lohmann *et al.*, 2001; Busch *et al.*, 2010; Moyroud *et al.*, 2011). However, several lines of evidence indicate that the joint activities of LFY and WUS are not sufficient to explain the induction of *AG*. First, the expression patterns of the three genes do not coincide. *WUS* is expressed in a small group of central cells in the deep layers of the meristem, the so-called organizing centre (Mayer *et al.*, 1998), while WUS protein can move to the upper layers of the floral meristem (Yadav *et al.*, 2011), and *LFY* is expressed throughout the floral bud (Blázquez *et al.*, 1997). In contrast, *AG* expression is specific to the interior two whorls of the flower. Second, *LFY* and *WUS* expression is detected in stage 1 flower buds, whereas *AG* transcripts are not detected until stage 3 (Busch *et al.*, 1999). Third, LFY and WUS factors are not sufficient to activate an *AG* reporter gene in a heterologous system (Lohmann *et al.*, 2001). Last, the presence of LFY is not absolutely required for *AG* expression, because *AG* transcripts are detected in a restricted domain at the centre of small flower buds in *lfy* loss-of-function mutants. Other regulators thus remain to be characterized to elucidate the mechanism by which *AG* expression is activated in a precise spatiotemporal pattern during flower development.

Additional players in the Arabidopsis floral stem cell termination process have been identified, among which are the ULT1 and ULT2 SAND domain-containing proteins (Fletcher, 2001; Carles *et al.*, 2005; Monfared *et al.*, 2013). Loss-of-function mutations in the *ULT1* gene produce supernumerary whorls correlating with a delay in *AG* activation in the centre of the flower meristem, indicating that ULT1 plays a major role in controlling floral determination, via the timely induction of *AG* expression. We showed that *AG* is a direct target of transcriptional activation by the ULT1 protein (Carles and Fletcher, 2009). Interestingly, *ULT1* and *AG* expression patterns overlap in the centre of the developing flower and *ULT1* transcripts are detected one stage earlier than *AG* transcripts, at stage 2 (Yanofsky *et al.*, 1990; Carles *et al.*, 2005; Carles and Fletcher, 2009).

ULT1 harbours a trithorax group (trxG) type of function that is antagonistic to PcG function, both genetically and molecularly. ULT1 loss-of-function mutations rescue the PcG chromatin modifier CURLY LEAF (CLF) loss-of-function phenotypes and ULT1 represses the deposition of PcG-induced repressive chromatin marks on lysine 27 of histone 3 (H3K27me3) in the floral MADS box loci (Carles and Fletcher, 2009). Moreover, ULT1 physically interacts with ARABIDOPSIS TRITHORAX 1 (ATX1), a chromatin modifier that functions in both assembly of the pre-initiation complex (PIC) and deposition of active chromatin marks on lysine 4 of histone 3 (H3K4me3) (Ding *et al.*, 2011). ULT1 thus stands as an activator of *AG* and other MADS box genes, which functionally relates it to LFY. Moreover, it is a good candidate to fill the gap in explaining the specific spatial and temporal activation of *AG*.

In this study, we analysed the genetic interaction between ULT1 and LFY during flower formation and showed that double mutants carrying ULT1 and LFY loss-of-function alleles displayed synergistic phenotypes. We also found that LFY was not required for ULT1-mediated *AG* activation and that ULT1 was not necessary for LFY gain-of-function phenotypes or LFY-mediated activation of several developmental target genes. Together, our data reveal that ULT1 and LFY function in independent pathways for regulating organogenesis and for activating *AG* expression in the centre of the developing flower to terminate floral meristem activity.

MATERIALS AND METHODS

Plant material and growth conditions

The *ult1-1*, *ult1-2*, *lfy-5* and *lfy-6* alleles were previously isolated from ethyl methanesulphonate mutagenesis populations on the Landsberg *erecta* (L*er*) background of *Arabidopsis thaliana* (Weigel *et al.*, 1992; Fletcher, 2001). The *ult1-3* allele corresponds to a Col-0 T-DNA insertion described previously (Carles *et al.*, 2005). The L*er* accession, to which all mutants were backcrossed at least three times, was used as the wild-type (WT) strain for all analyses. Plants were grown in a 1:1:1 mixture of perlite:vermiculite:topsoil under continuous cool white fluorescent lights (120 μmol m^{-2} s^{-1}) at 21 °C. For the *CaMV35S::LFY* experiments, plants were grown in long-day conditions (16 h light, 8 h

darkness) under cool white fluorescent lights (100 μmol m^{-2} s^{-1}), at 21 °C, on a 1:1 mixture of soil:vermiculite. Plants of the T_2 generation used for reverse transcription (RT)-PCR were grown for 7 d on Murashige and Skoog medium (Sigma) supplemented with 0·3 % sucrose (MS medium).

Constructs for transgenic plants

The *CaMV35S::ULT1* and *CaMV35S::LFY* constructs, allowing expression of the full-length *ULT1* or *LFY* coding sequence, have been described previously (Carles and Fletcher, 2009; Chahtane *et al.*, 2013). *Agrobacterium tumefaciens* EHA105 (for the *CaMV35S::ULT1* construct) or C58 pMP90 (for the *CaMV35S::LFY* construct) was used for stable transformation of WT, *ult1* homozygous or *lfy-6* heterozygous plants. Transgenic lines were generated by the floral dip method (Clough and Bent, 1998) and selected on MS plates containing 100 μg ml^{-1} gentamicin (for the *CaMV35S::ULT1* construct) or selected for green fluorescent protein (GFP) fluorescence in the seed coat (for the *CaMV35S::LFY* construct, due to the presence of the At2S3::GFP marker), under an epifluorescence dissecting microscope.

Gene expression analysis

Total RNA was isolated from 50 mg of inflorescences or leaves of recently bolted plants grown on soil (Figs 1 and 2) or from 7-day-old seedlings grown on MS medium (Fig. 3), using the RNeasy plant kit (Qiagen), treated with RNase-free DNase I (Roche) for 20 min at 37 °C and then purified with phenol/chloroform. RNase treatment of samples in Fig. 3 was performed with the DNA-*free*™ kit (Ambion) according to the manufacturer's instructions.

First-strand cDNA synthesis was performed with 5 μg (Figs 1 and 2) or 2 μg (Fig. 3) of total RNA using Superscript III Reverse Transcriptase (Life Technologies) and an oligo dT primer (18mer) according to the manufacturer's instructions. From 20 μl of the RT product, 1 μl was used for each PCR reaction. The annealing temperature was 54 °C for all primer pairs and 30 cycles of PCR were performed for *ULT1*, *AG*, *LFY*, *AP1* and *TEL2*, 32 cycles for *AP3* and 25 cycles for *LFY* and *EF1*α (RT-PCR results are presented in Figs 2 and 3 and Supplementary Data Fig. S2). For quantification of *AG* and *AP3* cDNAs by real-time PCR (Fig. 1), we used SYBR Green PCR Master Mix (Applied Biosystems) and an ABI 7000 Thermocycler (Applied Biosystems). The specificity of amplification was determined by dissociation curve analysis. Three technical replicates were done for each sample. Relative quantification (RQ) values were calculated using the $2^{-\Delta Ct}$ method (Livak and Schmittgen, 2001). The ΔCt was calculated using the *EF1*α gene as the endogenous control. Values given in Fig. 1G represent the RQ average of three biological replicates, with the RQ of WT set at 100 %. Primer sequences are listed in Carles and Fletcher (2009) and Chahtane *et al.* (2013), except for *TEL2* (forward 5′-CCATTATTATCCACCGCCACCACCACCATCACGAATGG-3′, reverse 5′-ACTCCTGCTAGCCTAACGTTCTTG-3′) and *AP1* (forward 5′-GCACATCCGCATAGAAAAAACCAAC-3′, reverse 5′-CTTCTTGATACAGACCACCCATG-3′). RNA *in situ* hybridization using an *AG* antisense probe was performed as previously described (Carles and Fletcher, 2009).

RESULTS

Synergistic phenotypes of ult lfy *double mutants*

Because ULT1 and LFY have overlapping functions in flower development, we addressed the question of whether they interacted genetically by analysing the flower phenotypes of *ult1 lfy* double mutants. Double mutants were constructed from two loss-of-function alleles for each gene: the dominant negative *ult1-1* allele and the null *ult1-2* allele on one hand, and the weak *lfy-5* allele and strong *lfy-6* allele on the other hand (Weigel *et al.*, 1992; Fletcher, 2001).

Loss of ULT1 function caused overproliferation of flowers and floral organs (Fig. 1A, D and Fletcher, 2001). In *ult1* flowers the number of organs in each whorl was increased (Fletcher, 2001), correlating with enlargement of the *WUS* expression domain. Moreover, the number of whorls varied from four to six, correlating with a delay in *AG* activation in the centre of the flower (Fletcher, 2001; Carles *et al.*, 2004, 2005). The floral organ number increase was more moderate in *ult1-2* flowers than in *ult1-1* flowers, which resembled *ult1 ult2* flowers (Monfared *et al.*, 2013). Thus, ULT1 functions in limiting floral meristem activity and promoting floral determinacy.

The *lfy-6* mutant allele, as one of the most severe LFY alleles, revealed the key role of LFY in the specification of floral meristem identity. Indeed, *lfy-6* flowers were replaced by cauline leaves with meristematic structures developing at their axils that gave rise to shoots or shoot/flower intermediates, revealing flower determinacy defects (Fig. 1B and Weigel *et al.*, 1992). The weaker *lfy-5* allele produced flowers with reduced numbers of petals and stamens as well as mosaic petal/stamen organs (Supplementary Data Fig. S1O, and Weigel *et al.*, 1992), thus revealing a function for LFY in the specification of floral organ identity in whorls 2 and 3. This function was largely masked in *lfy-6* plants because most *lfy-6* floral structures have shoot characteristics (Schultz and Haughn, 1991; Weigel *et al.*, 1992). These defects in flower and floral organ identity correlate with loss of MADS box floral gene expression (Weigel and Meyerowitz, 1993).

Flowers of plants with the *lfy-6* strong allele exhibited characteristics normally associated with secondary inflorescence shoots: flowers were often subtended by floral bracts, structures morphologically similar to the cauline leaves, usually subtending secondary inflorescence shoots. Flowers of the *lfy-6* strong allele exhibited outermost organs with cauline leaf-like features while the more internal organs were sepal-like, or mosaic sepal/carpel structures (Fig. 1E). Later during inflorescence development, the flowers in the axils of the bracts could be absent or aborted, then appeared as filamentous structures (Schultz and Haughn, 1991; Weigel *et al.*, 1992; Supplementary Data Fig. S1G, J, K).

The flower and floral organ identity defects of *lfy-6* single mutants appeared enhanced when combined with *ult1* mutations. The primary inflorescence meristems of *ult1-1 lfy-6* double mutants produced many *lfy*-like secondary inflorescence meristems, which were subtended by cauline leaves (Fig. 1C), followed by a small number of flowers. Thus, *ult1-1 lfy-6* inflorescence meristems appeared to have less floral character than *lfy-6* meristems (Fig. 1B). The flowers of *ult1-1 lfy-6* double mutants contained extra sepal-like organs in the first whorl, or reiterative sepal-bracts within the outer whorl organs,

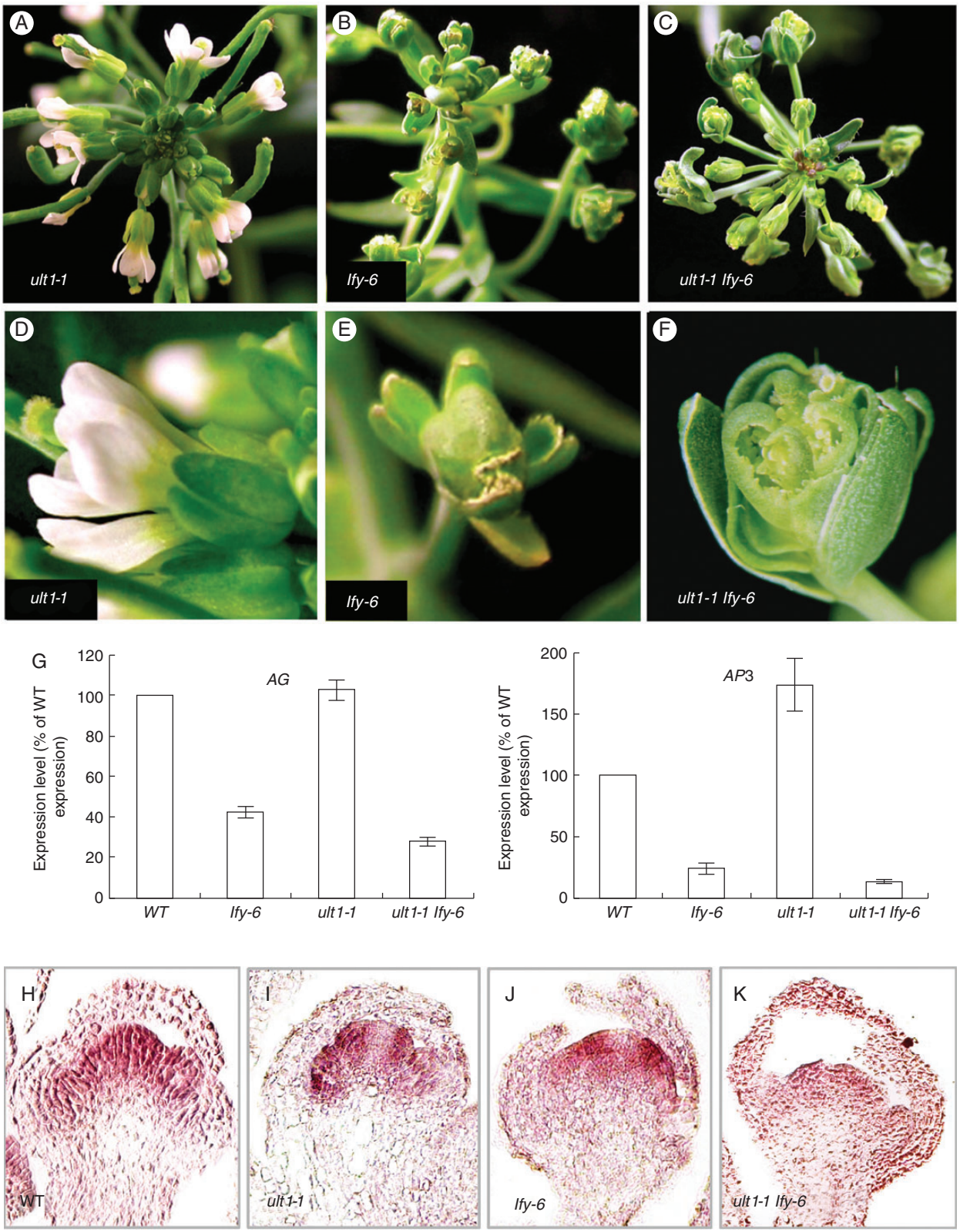

FIG. 1. ULT1 and LFY pathways are synergistic for floral meristem determinacy and for *AGAMOUS* and *APETALA3* regulation. Inflorescence (A–C) and flower (D–F) phenotypes of *ult1* and *lfy* single- and double-mutant plants. (A, D) *ult1-1*, (B, E) *lfy-6*, (C, F) *ult1-1 lfy-6*. (G) *AGAMOUS* (*AG*) and *APETALA3* (*AP3*) expression levels in WT, *ult1-1*, *lfy-6* and *ult1-1 lfy-6* inflorescences. Graphs represent average values from three biological replicates, each standardized to *EF1α*, with the value for the WT background set at 100 %. Error bars represent standard errors. Differences between *AG* and *AP3* expression levels in *lfy-6* and *ult1-1 lfy-6* flowers are statistically significant ($P < 0{\cdot}05$, Student's *t*-test). (H–K) *AG* mRNA expression pattern in (H) WT, (I) *ult1-1*, (J) *lfy-6*, (K) and *ult1-1 lfy-6* stage 6 flowers.

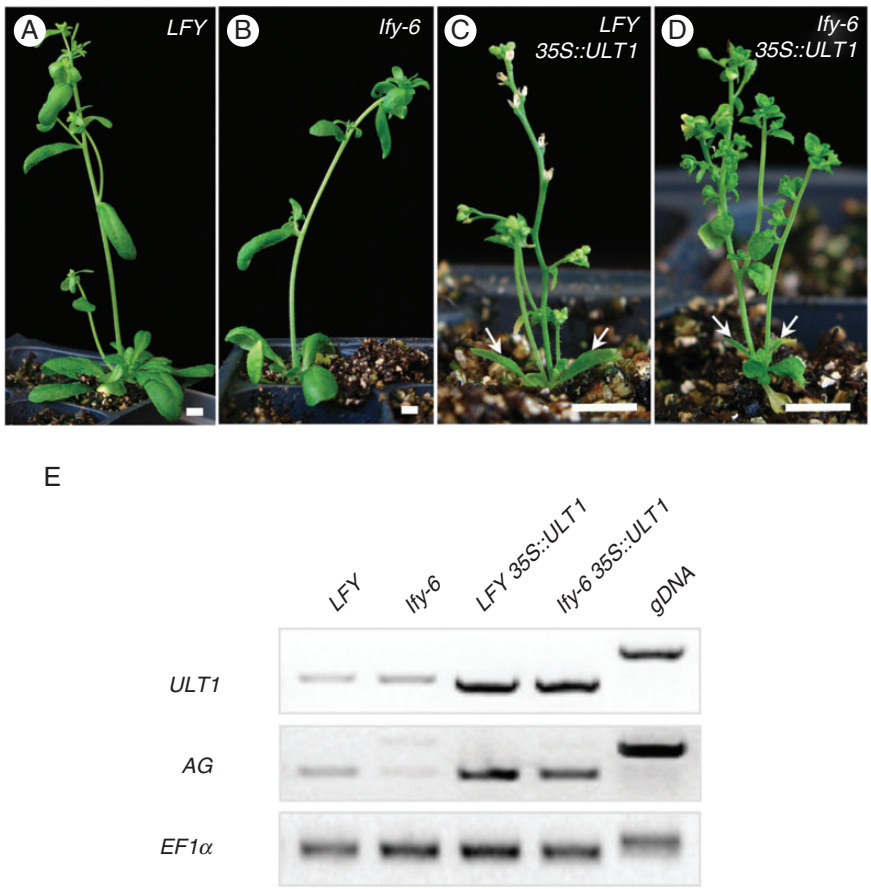

FIG. 2. Ectopic activation of *AG* by ULT1 is independent of LFY. (A–D) Phenotypes of *lfy-6* plants containing the *CaMV35S::ULT1* construct. Images are of plants segregating from a *lfy-6/+ 35S::ULT1* primary transformant with a severe (class 1) phenotype. (A) *LFY* WT plant, (B) *lfy-6* plant, (C) *LFY* WT *CaMV35S::ULT1* plant, (D) *lfy-6 CaMV35S::ULT1* plant. Scale bar = 0·5 cm. Arrows indicate upward-curled leaves. (E) RT-PCR analysis of *ULT1* and *AG* expression in leaves of the plants pictured in (A–D). *EF1α* was used as internal control. gDNA, genomic DNA template.

and multiple carpeloid structures in the centre (Fig. 1F). Thus, the flower to inflorescence meristem conversion appeared more complete in *ult1-1 lfy-6* double mutants than in *lfy-6* single mutants. In *ult1-2 lfy-6* plants, the primary inflorescence produced a few flowers and numerous small, tendrilous filamentous structures before undergoing termination (Supplementary Data Fig. S1I, K). The *ult1-2 lfy-6* flowers that formed consisted of floral organs that were strongly leaf-like in the outer whorls and carpeloid in the centre (Supplementary Data Fig. S1F), similar to *ult1-1 lfy-6* flowers.

Flower meristem identity was largely normal in *lfy-5* plants, which distinguished this allele from *lfy-6* (Weigel *et al.*, 1992; Supplementary Data Fig. S1A, D, L, O). The *ult1-1 lfy-5* double mutants had an enhanced *lfy-5* like phenotype, with flower meristems partially converted into inflorescence meristems that formed secondary flowers in the axils of the first whorl bract/leaf/sepal-like organs (Supplementary Data Fig. S1M, P, S). The double-mutant plants also produced many secondary and tertiary inflorescence meristems subtended by cauline leaves.

With respect to floral organ identity, flowers of the *lfy-5* weak mutant allele formed more organs with petal and stamen sectors, and more nearly normal petals and stamens, than *lfy-6* flowers (Weigel *et al.*, 1992). In *ult1-2 lfy-5* double mutants, the *lfy-5* floral organ identity defects were enhanced towards *lfy-6* phenotypes (Supplementary Data Fig. S1Q). The flowers were more leaf-like than *lfy-5* flowers, but still produced petals and stamens.

Additionally, in the *ult1 lfy-5* and *ult1 lfy-6* double mutants, the inflorescences produced lateral structures in larger numbers than in *lfy* single mutants and the flowers carried extra sepal-like organs in the first whorl, which is characteristic of *ult1* loss-of-function phenotypes (Supplementary Data Fig. S1E, F, P, Q). Moreover, *ult1-1 lfy-6* and *ult1-1 lfy-5* double-mutant flowers showed enhanced loss of determinacy compared with *lfy-6* and *lfy-5* single-mutant flowers, producing many extra whorls of carpels or sepal/carpel-like organs (Fig. 1E–F, Supplementary Data Fig. S1E, P).

We conclude from the genetic interaction analyses that *ult1 lfy* double-mutant flowers produced many more sepal/bract/leaf-like organs than *lfy* single mutant flowers. Moreover, floral meristem identity in the double mutants was highly converted towards inflorescence meristem identity during early reproductive development, as revealed by the introduction of *ult1* mutations into the weak *lfy-5* background. Consistently, although carpels still developed in *ult1 lfy* double mutant flowers, they occurred in many additional floral whorls, demonstrating that *ult1*-related loss of floral determinacy was largely enhanced on a *lfy-5* or *lfy-6* background. In general, the *ult1* and *lfy*

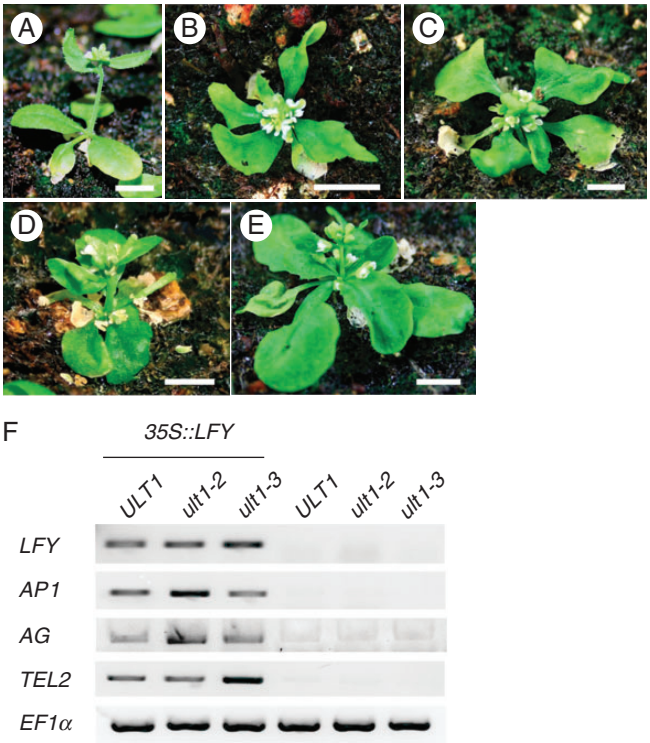

FIG. 3. LFY overexpression phenotypes and ectopic activation of *AP1*, *AG* and *TEL2* by LFY are independent of ULT1. (A–E) Phenotypes of L*er* WT and *ult1-3* plants carrying the *CaMV35S::LFY* construct. (A) L*er* WT untransformed plant. (B) ULT1 *CaMV35S::LFY* plant with a severe (class a) phenotype, producing ectopic rosette flowers and lacking stem elongation. (C) *ult1-3 CaMV35S::LFY* plant with a class a phenotype. (D) ULT1 *CaMV35S::LFY* plant with a less severe (class b) phenotype, producing ectopic rosette flowers and an elongated stem. (E) *ult1-3 CaMV35S::LFY* plant with a class b phenotype. Scale bar = 1 cm. (F) RT-PCR analysis of *LFY*, *AP1*, *AG* and *TEL2* expression in 7-day-old ULT1 WT, *ult1-2* and *ult1-3* seedlings that either contained or lacked the *CaMV35S::LFY* construct. *EF1α* was used as internal control.

single-mutant phenotypes were enhanced in the double mutants, indicating separate, parallel regulatory pathways for the two corresponding functions.

In order to further evaluate the action of ULT1 and LFY in independent floral pathways, we analysed *AG* expression levels in *ult1 lfy* flowers by RT-qPCR and the *AG* expression pattern by RNA *in situ* hybridization. We found that *AG* expression levels were significantly reduced in *ult1-1 lfy-6* inflorescences compared with *lfy-6* inflorescences (Fig. 1G). Transcripts from the *AP3* gene, another LFY and ULT1 target, were also significantly reduced (Fig. 1G).

Expression levels of *AP3* were higher in *ult1* inflorescences than in WT inflorescences, which could be explained by the fact that *ult1-1* inflorescences produce many more flowers than WT inflorescences, thus increasing the ratio of whorl 2 and 3 founder cells relative to total inflorescence cells in the sampled tissues. RNA *in situ* hybridization experiments showed an absence of *AG* expression in the centre of both *ult1-1* and *lfy-6* stage 6 floral meristems (Fig. 1I, J) compared with WT floral meristems (Fig. 1H), whereas the detection signal for *AG* transcripts was even weaker in *ult1-1 lfy-6* floral meristems (Fig. 1 K). Together, this expression dataset supports independent functions for ULT1 and LFY in regulating flower determinacy, via *AG* activation.

LFY is not necessary for ULT1-mediated AG activation

When ectopically expressed in Arabidopsis, ULT1 causes strong developmental defects, such as production of small rosettes carrying upward-curled leaves, early bolting and bushy plant features, as well as inflorescences terminating early into compact structures with mosaic floral organs. We previously showed that, in these *CaMV35S::ULT1* lines, ULT1 activates the ectopic expression of a number of floral MADS box genes, including *AG*, which is also a target of LFY induction (Carles and Fletcher, 2009). Indeed, the developmental phenotypes are largely due to the ectopic activity of AG (Carles and Fletcher, 2009). In order to test whether activation of target genes by ULT1 requires LFY function, we transformed a population of *lfy-6*/+ plants with the *CaMV35S::ULT1* construct (Carles and Fletcher, 2009). We analysed the phenotypes of 64 primary transformants, among which were 11 plants homozygous for the *lfy-6* mutation. Of the transformants obtained on a *LFY* or *lfy-6*/+ background, 11·3 % showed strong *ULT1* ectopic expression phenotypes (class 1), with small rosettes carrying upward-curled leaves, bolting early and developing into a short, bushy structure (Fig. 2A–D; Supplementary Data Fig. S2). An additional 24·5 % displayed intermediate phenotypes (class 2), displaying less severe leaf curling, early flowering and bushiness than class 1 plants. The remaining 64·2 % showed a WT phenotype (class 3). The distribution of phenotypic classes observed in transformants on the *lfy-6* background was similar to that of transformants on the *LFY* or *lfy-6*/+ background, with 9·1 % of the *lfy-6* transformants displaying class 1 phenotypes, 18·2 % displaying class 2 phenotypes and 72·7 % displaying class 3 phenotypes (Supplementary Data Fig. S2). These results indicate that LFY function may not be required for ectopic activation/de-repression of ULT1 target genes. To address this question, we analysed the expression of *AG* in *lfy-6 CaMV35S::ULT1* leaves by RT-PCR. We found that ULT1-induced *AG* ectopic expression was not affected by the loss of LFY function, indicating that *AG* transactivation by ULT1 is independent of LFY (Fig. 2E).

ULT1 is not necessary for LFY gain-of-function phenotypes and LFY-mediated target gene activation

When constitutively expressed in Arabidopsis LFY is sufficient to induce floral fate in lateral shoot meristems (Weigel and Nilsson, 1995). This phenotype is partly dependent on the function of the *APETALA1* (*AP1*) gene, which is ectopically activated in *CaMV35S::LFY* plants. Several other target genes are also induced in *CaMV35S::LFY* seedling tissues, including the *TERMINAL EAR LIKE 2* (*TEL2*) gene, which is proposed to function in meristem maintenance (Chahtane *et al.*, 2013).

In order to test whether activation of target genes by LFY requires ULT1 function, we analysed the phenotypes of *CaMV35S::LFY* lines on an *ult1* null mutant background (Fig. 3). We examined 14 T_1 transformants on the L*er* background and 42 transformants on the *ult1-3* background. Of the transformants on the L*er* background, 14·3 % displayed strong phenotypes (class a) previously associated with ectopic *LFY* expression (Fig. 3), including the formation of ectopic flowers in the axils of rosette leaves (rosette flowers) and compact stems lacking internode elongation (Weigel and Nilsson, 1995;

Chahtane *et al.*, 2013). An additional 57·1 % displayed intermediate phenotypes (class b) consisting of rosette flowers only. The remaining 28·6 % showed a WT phenotype (class c; Supplementary Data Fig. S3). The distribution of phenotypic classes observed on the *ult1-3* background was slightly shifted towards stronger phenotypes, but this difference was not significant (Supplementary Data Fig. S3). Of these transformants, 28·6 % displayed class a phenotypes, 64·3 % displayed class b phenotypes, and 7·1 % displayed class c phenotypes. These results suggest that LFY does not seem to require ULT1 function to perform its action.

To analyse whether, as suggested by the morphological data, LFY can still activate its target genes in the absence of ULT1, we performed RT-PCR on 7-day-old T_2 seedlings obtained from transformation of the *CaMV35S::LFY* construct onto the L*er* WT, *ult1-2* or *ult1-3* mutant backgrounds. Expression of the LFY target genes *AP1*, *AG* and *TEL2* was nearly undetectable in untransformed WT, *ult1-2* and *ult1-3* seedlings (Fig. 3F). However, in *CaMV35S::LFY* seedlings with an intermediate phenotype (class b), ectopic expression of *AP1*, *AG* and *TEL2* correlated with *LFY* ectopic expression on all analysed backgrounds (ULT1 WT, *ult1-2* and *ult1-3* mutant). Moreover, expression of the target genes was elevated by *CaMV35S::LFY* to the same extent on the WT background as on *ult1* mutant backgrounds (Fig. 3F). These results show that loss of ULT1 function has no effect on ectopic activation of these two developmentally important target genes by LFY.

DISCUSSION

ULT1 and LFY interactions

In genetic interaction tests, we found that double mutants for ULT1 and LFY loss-of-function alleles display additive flower identity and synergistic determinacy phenotypes, indicating that the two factors function independently in these processes. ULT1 and LFY both control the expression of the *AG* gene, the activation of which is required for flower meristem termination. Loss-of-function and gain-of-function experiments together with molecular analyses show that ULT1 and LFY function independently in *AG* regulation. In a similar manner, LFY can activate downstream target genes that regulate flower meristem identity, independently of ULT1 function.

LFY has long been recognized as a key regulator of *AG* expression in developing flowers (Busch *et al.*, 1999). Yet *AG* transcripts can be detected in *lfy* null mutant flowers, demonstrating that *AG* can be induced independently of LFY (Weigel and Meyerowitz, 1993; Lenhard *et al.*, 2001). Our finding that ULT1 does not require LFY function to activate *AG* expression in plant tissues suggests that ULT1 is one factor that can mediate LFY-independent *AG* induction during flower formation.

CaMV35S::ULT1 lines on a LFY WT background develop upward-curled leaves, bolt early and develop flowers with homeotic transformation of sepals and petals into stamenoid and carpelloid structures. We previously showed that these phenotypes are mostly due to *AG* ectopic function (Carles and Fletcher, 2009). Here we found that *CaMV35S::ULT1 lfy-6* plants produced upward-curled leaves, indicating that ectopic *AG* transcripts are functional in this tissue. This contrasts with the lateral structures emerging from the inflorescence meristems in which, although *AG* was ectopically activated, no organs with floral identity developed, and hence no ectopic stamen or carpel structures. This indicates that in *CaMV35S::ULT1* plants LFY, while not required for the transcriptional activation of the *AG* gene, is needed for the function of the ectopic *AG* transcripts in the flower. This is reminiscent of previous observations showing that ULT1 function is required for the function of *AG* ectopic transcripts in *CaMV35S::AG* transgenic lines (Carles and Fletcher, 2009). It is possible that LFY, like ULT1, is required for translation of *AG* transcripts into proteins or for the function of the AG protein in the flower.

LFY directly and specifically interacts with target genes in which specific DNA binding sequences were identified (Moyroud *et al.*, 2011; Winter *et al.*, 2011). Direct association of ULT1 protein with target loci has been shown by chromatin immunoprecipitation followed by quantitative PCR (ChIP-qPCR) (Carles and Fletcher, 2009), and the protein contains a SAND domain that in animal homologues acts as a sequence-specific DNA binding domain (Bottomley *et al.*, 2001; Surdo *et al.*, 2003). However, although ULT1 protein shows general affinity for DNA, Selex, protein binding microarrays and electromobility shift assay experiments failed to identify specific DNA binding motifs (data not shown). Whether ULT1 therefore requires additional protein partners or a specific chromatin context in order to interact with DNA in a sequence-specific manner remains to be resolved.

Model of ULT1 function in flower meristem determinacy

Previous molecular analysis of ULT1 loss- and gain-of-function lines (Fletcher, 2001; Carles *et al.*, 2004, 2005; Carles and Fletcher, 2009), together with this study, allow us to propose a model in which ULT1 is a space and time determinant for *AG* induction in the centre of the flower and a component of the later repression of *WUS* expression (Fig. 4), thus leading to the termination of the floral meristem. We postulate that ULT1, in

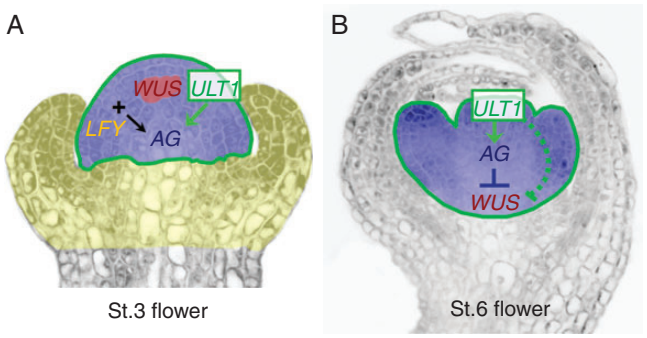

FIG. 4. Model of ULT1 function in floral meristem termination. (A) At stage 3 of flower development, ULT1 is required in a pathway independent of WUS and LFY to provide the requisite spatial and temporal induction of *AG* expression in the centre of the floral meristem. (B) ULT1 activity, through both *AG* activation (arrow) and an AG-independent repressive pathway (dotted line), contributes to the termination of *WUS* expression at stage 6. The *WUS* expression domain is represented by red shading, the *AG* expression domain by blue shading, the *ULT1* expression domain is outlined in green and the *LFY* expression domain, which spans the expression domains of the other three genes, is represented by yellow shading.

a pathway independent of LFY and WUS, activates *AG* expression in the centre of the stage 3 floral meristem (Fig. 4A). As flower development continues, ULT1 activity through AG activation, as well as an AG-independent pathway via SUPERMAN (Prunet *et al*., 2008), contributes to the extinction of *WUS* expression at stage 6 (Fig. 4B).

This model is consistent with multiple independent lines of evidence. First, *ULT1* expression precedes expression of *AG* in flower primordia and the expression patterns of the two genes overlap: *ULT1* transcripts are detected throughout the floral meristem beginning at stage 2 and become restricted to the centre of the floral meristem at stage 3 (Carles *et al*., 2005), when *AG* expression is first detected in the same domain (Yanofsky *et al*., 1990). Second, flower meristem termination is delayed in *ult1* mutants, correlating with a delay in *AG* expression in the centre of the floral meristem (Fletcher, 2001). Third, ectopic ULT1 activity leads to ectopic activation of *AG* (Carles and Fletcher, 2009). Fourth, *ult1* and *lfy* loss-of-function mutant phenotypes are synergistic for flower determinacy (this study), and ULT1 can activate *AG* expression independently of LFY (this study). Finally, *wus* is epistatic to *ult1* in the centre of the flower and *WUS* transcriptional repression is delayed in *ult1* floral meristems (Carles *et al*., 2004).

According to our model, LFY and WUS transcription factors would render the *AG* locus transcriptionally active via specific DNA sequence recognition, whereas ULT1 would confer temporal and spatial specificity on the activation. LFY and WUS have overlapping DNA binding sites in the second intron of *AG* (Busch *et al*., 2010), and LFY also binds to several sites in the promoter (Moyroud *et al*., 2011; Winter *et al*., 2011). ULT1 likewise associates *in vivo* with *AG* regulatory sites located in its second intron, as well as in its promoter-proximal region (Carles and Fletcher, 2009). Interestingly, these ULT1 binding regions overlap with the LFY binding regions, although whether ULT1 associates with exactly the same regulatory sequences as LFY and WUS at the *AG* locus, or has a broader interaction pattern with local DNA/nucleosomes, remains to be resolved.

Our evidence to date suggests that the association of ULT1 with the *AG* regulatory region leads to chromatin modifications at the locus. We previously showed that ULT1 induces de-repression of *AG* and *AP3* target genes by removal of PcG-mediated H3K27me3 chromatin repressive marks (Carles and Fletcher, 2009). We also found that ULT1 physically interacts with ATX1, an Arabidopsis trxG factor that functions in PIC formation as well as in the deposition of activating H3K4me3 marks at developmental target genes such as *AG*. One reasonable hypothesis is that ULT1 would interact with or recruit ATX1 in cells at the centre of stage 3 floral meristems for PIC formation at the *AG* locus. The independent contributions of the ULT1-mediated chromatin-modifying complex and the LFY–WUS transcription factors would thus bring about a switch at the *AG* locus from an inactive to an active transcriptional state at the correct place and time during flower development.

SUPPLEMENTARY DATA

Supplementary data are available online at www.aob.oxfordjournals.org and consist of the following. Figure S1: illustration of phenotypes of *ult1 lfy* double mutants. Figure S2: phenotypic distribution of T_1 lines containing the 35S::*ULT1* construct. Figure S3: phenotypic distribution of T_1 lines containing the 35S::*LFY* construct.

ACKNOWLEDGEMENTS

This work was supported by the French Ministry of Foreign Affairs (French Embassy stipend to J.E.), the Rhône-Alpes county (Allocation Doctorale de Recherche, Cluster 7, 12–01293101 to F.M.), the University of Grenoble-Alpes (UGA-UJF), the Centre National de la Recherche Scientifique (CNRS-Higher Education Chair, position 0428–64 to C.C.C.) and the US National Science Foundation (IBN0110667 to J.C.F).

LITERATURE CITED

Blázquez MA, Soowal LN, Lee I, Weigel D. 1997. LEAFY expression and flower initiation in Arabidopsis. *Development* **124**: 3835–3844.

Bottomley MJ, Collard MW, Huggenvik JI, Liu Z, Gibson TJ, Sattler M. 2001. The SAND domain structure defines a novel DNA-binding fold in transcriptional regulation. *Nature Structural Biology* **8**: 626–633.

Busch MA, Bomblies K, Weigel D. 1999. Activation of a floral homeotic gene in Arabidopsis. *Science* **285**: 585–587.

Busch W, Miotk A, Ariel FD, *et al*. 2010. Transcriptional control of a plant stem cell niche. *Developmental Cell* **18**: 849–861.

Carles CC, Fletcher JC. 2009. The SAND domain protein ULTRAPETALA1 acts as a trithorax group factor to regulate cell fate in plants. *Genes & Development* **23**: 2723–2728.

Carles CC, Lertpiriyapong K, Reville K, Fletcher JC. 2004. The ULTRAPETALA1 gene functions early in Arabidopsis development to restrict shoot apical meristem activity and acts through WUSCHEL to regulate floral meristem determinacy. *Genetics* **167**: 1893–1903.

Carles CC, Choffnes-Inada D, Reville K, Lertpiriyapong K, Fletcher JC. 2005. ULTRAPETALA1 encodes a SAND domain putative transcriptional regulator that controls shoot and floral meristem activity in Arabidopsis *Development* **132**: 897–911.

Chahtane H, Vachon G, Le Masson M, *et al*. 2013. A variant of LEAFY reveals its capacity to stimulate meristem development by inducing RAX1. *Plant Journal* **74**: 678–689.

Clough SJ, Bent AF. 1998. Floral dip: a simplified method for *Agrobacterium*-mediated transformation of *Arabidopsis thaliana*. *Plant Journal* **16**: 735–743.

Ding Y, Avramova Z, Fromm M. 2011. Two distinct roles of ARABIDOPSIS HOMOLOG OF TRITHORAX1 (ATX1) at promoters and within transcribed regions of ATX1-regulated genes. *Plant Cell* **23**: 350–363.

Ditta G, Pinyopich A, Robles P, Pelaz S, Yanofsky MF. 2004. The SEP4 gene of *Arabidopsis thaliana* functions in floral organ and meristem identity. *Current Biology* **14**: 1935–1940.

Fletcher JC. 2001. The ULTRAPETALA gene controls shoot and floral meristem size in Arabidopsis. *Development* **128**: 1323–1333.

Irish VF. 2010. The flowering of Arabidopsis flower development. *Plant Journal* **61**: 1014–1028.

Krizek BA, Fletcher JC. 2005. Molecular mechanisms of flower development: an armchair guide. *Nature Reviews Genetics* **6**: 688–698.

Laux T, Mayer KF, Berger J, Jürgens G. 1996. The WUSCHEL gene is required for shoot and floral meristem integrity in Arabidopsis. *Development* **122**: 87–96.

Lenhard M, Bohnert A, Jürgens G, Laux T. 2001. Termination of stem cell maintenance in Arabidopsis floral meristems by interactions between WUSCHEL and AGAMOUS. *Cell* **105**: 805–814.

Liu X, Kim YJ, Müller R, *et al*. 2011. AGAMOUS terminates floral stem cell maintenance in Arabidopsis by directly repressing WUSCHEL through recruitment of Polycomb Group proteins. *Plant Cell* **23**: 3654–3670.

Livak KJ, Schmittgen TD. 2001. Analysis of relative gene expression data using real-time quantitative PCR and the $2^{-\Delta\Delta Ct}$ method. *Methods* **25**: 402–408.

Lohmann JU, Hong RL, Hobe M, *et al*. 2001. A molecular link between stem cell regulation and floral patterning in Arabidopsis. *Cell* **105**: 793–803.

Mayer KF, Schoof H, Haecker A, Lenhard M, Jürgens G, Laux T. 1998. Role of WUSCHEL in regulating stem cell fate in the Arabidopsis shoot meristem. *Cell* **95**: 805–815.

Monfared MM, Carles CC, Rossignol P, Pires HR, Fletcher JC. 2013. The ULT1 and ULT2 trxG genes play overlapping roles in Arabidopsis development and gene regulation. *Mol Plant* **6**: 1564–1579.

Moyroud E, Minguet EG, Ott F, *et al*. 2011. Prediction of regulatory interactions from genome sequences using a biophysical model for the Arabidopsis LEAFY transcription factor. *Plant Cell* **23**: 1293–1306.

O'Maoiléidigh DS, Graciet E, Wellmer F. 2013. Gene networks controlling *Arabidopsis thaliana* flower development. *New Phytologist* **201**: 16–30.

Parcy F, Nilsson O, Busch MA, Lee I, Weigel D. 1998. A genetic framework for floral patterning. *Nature* **395**: 561–566.

Pelaz S, Ditta GS, Baumann E, Wisman E, Yanofsky MF. 2000. B and C floral organ identity functions require SEPALLATA MADS-box genes. *Nature* **405**: 200–203.

Prunet N, Morel P, Thierry A-M, *et al*. 2008. REBELOTE, SQUINT, and ULTRAPETALA1 function redundantly in the temporal regulation of floral meristem termination in *Arabidopsis thaliana*. *Plant Cell* **20**: 901–919.

Schultz EA, Haughn GW. 1991. LEAFY, a homeotic gene that regulates inflorescence development in Arabidopsis. *Plant Cell* **3**: 771–781.

Smaczniak C, Immink RGH, Angenent GC, Kaufmann K. 2012*a*. Developmental and evolutionary diversity of plant MADS-domain factors: insights from recent studies. *Development* **139**: 3081–3098.

Smaczniak C, Immink RGH, Muiño JM, *et al*. 2012*b*. Characterization of MADS-domain transcription factor complexes in Arabidopsis flower development. *Proceedings of the National Academy of Sciences of the USA* **109**: 1560–1565.

Sun B, Xu Y, Ng K-H, Ito T. 2009. A timing mechanism for stem cell maintenance and differentiation in the Arabidopsis floral meristem. *Genes & Development* **23**: 1791–1804.

Sun B, Looi L-S, Guo S, *et al*. 2014. Timing mechanism dependent on cell division is invoked by Polycomb eviction in plant stem cells. *Science* **343**: 1248559.

Surdo PL, Bottomley MJ, Sattler M, Scheffzek K. 2003. Crystal structure and nuclear magnetic resonance analyses of the SAND domain from glucocorticoid modulatory element binding protein-1 reveals deoxyribonucleic acid and zinc binding regions. *Molecular Endocrinology* **17**: 1283–1295.

Weigel D, Meyerowitz EM. 1993. Activation of floral homeotic genes in Arabidopsis. *Science* **261**: 1723–1726.

Weigel D, Nilsson O. 1995. A developmental switch sufficient for flower initiation in diverse plants. *Nature* **377**: 495–500.

Weigel D, Alvarez J, Smyth DR, Yanofsky MF, Meyerowitz EM. 1992. LEAFY controls floral meristem identity in Arabidopsis. *Cell* **69**: 843–859.

Winter CM, Austin RS, Blanvillain-Baufumé S, *et al*. 2011. LEAFY target genes reveal floral regulatory logic, cis motifs, and a link to biotic stimulus response. *Developmental Cell* **20**: 430–443.

Yadav RK, Perales M, Gruel J, Girke T, Jönsson H, Reddy GV. 2011. WUSCHEL protein movement mediates stem cell homeostasis in the Arabidopsis shoot apex. *Genes & Development* **25**: 2025–2030.

Yanofsky MF, Ma H, Bowman JL, Drews GN, Feldmann KA, Meyerowitz EM. 1990. The protein encoded by the Arabidopsis homeotic gene agamous resembles transcription factors. *Nature* **346**: 35–39.